sensors

MDPI

Article

Two-Dimensional Direction-of-Arrival Fast Estimation of Multiple Signals with Matrix Completion Theory in Coprime Planar Array

Haiyun Xu, Yankui Zhang, Bin Ba *, Daming Wang and Xiangzhi Li

National Digital System Engineering and Technological Research R&D Center, Zhengzhou 450001, China; xuhaiyun1995@163.com (H.X.); zhang_yk_2018@163.com (Y.Z.); wdm_wangdaming@163.com (D.W.); lixiangzhi2231@163.com (X.L.)

* Correspondence: xidianbabin@163.com; Tel.: +86-181-0383-6862

Received: 13 April 2018; Accepted: 25 May 2018; Published: 28 May 2018

Abstract: In estimating the two-dimensional (2D) direction-of-arrival (DOA) using a coprime planar array, the main issues are the high complexity of spectral peak search and the limited degree of freedom imposed by the number of sensors. In this paper, we present an algorithm based on the matrix completion theory in coprime planar array that reduces the computational complexity and obtains a high degree of freedom. The algorithm first analyzes the covariance matrix of received signals to estimate the covariance matrix of a virtual uniform rectangular array, which has the same aperture as the coprime planar array. Matrix completion theory is then applied to estimate the missing elements of the virtual array covariance matrix. Finally, a closed-form DOA solution is obtained using the unitary estimation signal parameters via rotational invariance techniques (Unitary-ESPRIT). Simulation results show that the proposed algorithm has a high degree of freedom, enabling the estimation of more signal DOAs than the number of sensors. The proposed algorithm has reduced computational complexity because the spectral peak search is replaced by Unitary-ESPRIT, but attains similarly high levels accuracy to those of the 2D multiple signal classification algorithm.

Keywords: direction-of-arrival; coprime planar array; matrix completion theory; degree of freedom

1. Introduction

Direction-of-arrival (DOA) estimation is a significant problem in many applications, such as radar [1], underwater acoustics [2], indoor navigation, and so on [3]. At present, most existing DOA techniques use the uniform and non-sparse arrays, including uniform line arrays (ULAs) [4], uniform rectangular arrays (URAs) [5] and uniform L-shaped arrays [6]. These require the distance between the nearest sensors to be no more than half the wavelength of the impinging signals, and use high-resolution subspace algorithms [7–10] to obtain accurate parameters. With the development of technology, the requirement for more precise location determination requires arrays with more sensors and expanded apertures. Unfortunately, this makes the systems more complicated, and enhances the antenna mutual coupling interference, which increases the estimation errors.

To acquire both high array degree of freedom and the required precision, researchers have begun to examine the signal features. For example, the array aperture has been expanded based on non-circular signals, whose ellipse covariance is non-zero [11], and a virtual array has been constructed in the frequency domain based on orthogonal frequency division multiplexing systems [12]. The algorithm in [12] not only improves the precision of parameters, but also estimates multiple targets (more than the number of sensors). Although the above studies make the best use of information, they are confined by the application environment. Hence, the sparse and non-uniform array structure was proposed.

The nested array in [13], which has a high freedom degree and precision, consists of a uniform and sparse array, and a uniform and non-sparse array. However, the nested array cannot avoid the mutual coupling interference among the sensors of the non-sparse array. Thus, a one-dimensional coprime array consisting of two uniform sparse line arrays was introduced in [14]. This weakens the mutual coupling interference, and simultaneously constructs a larger aperture with fewer sensors when compared with uniform and non-sparse arrays. The larger aperture obtains more precise estimates, and the $M + N - 1$ sensors can achieve $O(MN)$ degrees of freedom. Recently, two-dimensional (2D) coprime arrays and the corresponding DOA algorithms have been proposed [15–17]. The coprime planar array investigated in [15] has a complicated structure that could only be solved using the multiple signal classification (MUSIC) algorithm. As MUSIC uses a spectral peak search, the increase in accuracy is computationally expensive. A low complexity algorithm [16] has been applied to sparse L-shaped arrays. Although the number of signals that can be identified is limited to the number of sensors in these methods, parallel coprime subarrays have the ability to resolve $\left(M^2 - 1\right)/8$ signals with M sensors [17]. We will show that the proposed coprime planar arrays offer a higher degree of freedom than parallel coprime subarrays for the same number of sensors.

For DOA estimation using coprime planar arrays, the problems of high computational complexity and the inadequate array degree of freedom are overcome using an algorithm based on matrix completion theory. The method reconstructs the covariance matrix of the virtual uniform rectangular array, which is the same size as the coprime planar array, after analyzing the received signals' covariance matrix. We apply the matrix completion theory to estimate the missing elements of the covariance matrix. Using the unitary estimation signal parameters via rotational invariance techniques (Unitary-ESPRIT), we then realize the fast estimation of the 2D DOA angle. This algorithm ensures high precise estimation values, as it maintains the same aperture and avoids the spectral peak search, effectively reducing the complexity. The most important point is that increasing the number of virtual sensors enhances the degree of freedom, which allows us to find more signals than with existing methods.

The remainder of this paper is arranged as follows. Section 2 introduces the model of coprime planar array model, and Section 3 describes the steps of the algorithm. Sections 4 and 5 analyze the computational complexity and performance of the model, respectively, to demonstrate the validity of this algorithm. Section 6 gives the conclusion to this paper.

The notations used in this paper are as follows: I_N represents the N dimensional unit array; $(\bullet)^T$ and $(\bullet)^H$ respectively represent transposition and the conjugate transpose, respectively; $E(\bullet)$ denotes the mathematical expectation; $diag(\bullet)$ expresses the transformation of a vector to a diagonal matrix.

2. System Model

Considering the coprime planar array model introduced in [15], the array geometry is shown in Figure 1. The coprime planar array is made up of two URAs. Subarray 1 has $M_1 \times M_1$ sensors and subarray 2 has $M_2 \times M_2$ sensors, where M_1 and M_2 are the coprime integers (generally assuming $M_1 < M_2$) and denote the sensor numbers on the x, y axis. Correspondingly, the distance between the closest sensors is $M_2\lambda/2$ and $M_1\lambda/2$, respectively, where the λ represents the wavelength of the impinging signals. The subarrays coincide at the origin, so the total number of sensors is $M = M_1^2 + M_2^2 - 1$. Suppose that there are K uncorrelated narrowband far-field signals impinging on the array with the power $\{\sigma_1^2, \sigma_2^2, \cdots \sigma_K^2\}$. The kth signal is located at elevation angle θ_k, which is downward from the z-axis, and azimuth angle φ_k, which is counterclockwise from the x-axis.

We define the D_1 and D_2 as the location set of the subarrays. $D_1 = L_1\lambda/2$ and $D_2 = L_2\lambda/2$, where the $L_1 = \{(m,n)M_2, 0 \le m,n \le M_1 - 1\}$ and $L_2 = \{(m,n)M_1, 0 \le m,n \le M_2 - 1\}$. Hence,

the location set of the coprime planar array is expressed as $D = D_1 \cup D_2$ and we have $L = L_1 \cup L_2$. The received signals at the array can be represented as

$$X(t) = A(\varphi, \theta)S(t) + N(t) \tag{1}$$

The array manifold

$$A(\varphi, \theta) = \left[\begin{array}{cccc} a(\varphi_1, \theta_1) & a(\varphi_2, \theta_2) & \cdots & a(\varphi_K, \theta_K) \end{array} \right], \tag{2}$$

where

$$a(\varphi_k, \theta_k) = \left[\begin{array}{cccc} a_1(\varphi_k, \theta_k) & a_2(\varphi_k, \theta_k) & \cdots & a_M(\varphi_k, \theta_k) \end{array} \right]^T \tag{3}$$

$$a_m(\varphi_k, \theta_k) = e^{j\pi \sin\theta_k (x_m \cos\varphi_k + y_m \sin\varphi_k)}, (x_m, y_m) \in L \tag{4}$$

The signal data vector

$$S(t) = \left[\begin{array}{cccc} s_1(t) & s_2(t) & \cdots & s_K(t) \end{array} \right]^T, \tag{5}$$

where $t = 1, 2, \cdots J$ is the sampling time and J is the number of snapshots. And the noise vector

$$N(t) = \left[\begin{array}{cccc} n_1(t) & n_2(t) & \cdots & n_M(t) \end{array} \right]^T, \tag{6}$$

where the elements are usually Gaussian random variables with zero means and variance σ_n^2.

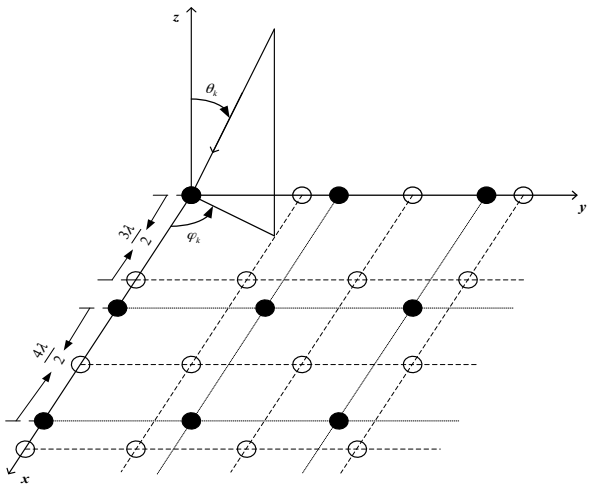

Figure 1. Geometry of coprime planar array when $M_1 = 3$, $M_2 = 4$.

3. The Proposed Algorithm

In [15], the DOA is estimated based on the two subarrays. Each subarray uses the subspace algorithm, but the results have some phase ambiguity. The two sets of results, including this ambiguity, have common values, and these are the real values. Therefore, the coprime planar array can be used to find DOAs. A partial spectral search (PSS) method is used to reduce the complexity caused by 2D-MUSIC mentioned in [15], but this does not significantly reduce the complexity.

3.1. Reconstructing the Covariance Matrix of the Virtual Array

Considering (1), the covariance matrix of the received signal is defined as

$$R_X = E\left[XX^H\right] = AR_SA^H + \sigma_n^2 I_M, \tag{7}$$

where $R_S = diag\left(\begin{array}{cccc}\sigma_1^2 & \sigma_2^2 & \cdots & \sigma_K^2\end{array}\right)$. We define $R = AR_SA^H$ and express the element in the mth row and nth column as

$$R_{m,n} = \sum_{k=1}^{K} \sigma_k^2 e^{j\pi \sin\theta_k((x_m - x_n)\cos\varphi_k + (y_m - y_n)\sin\varphi_k)} = R(x_m - x_n, y_m - y_n), \tag{8}$$

where the (x_m, y_m) is one element of set L. According to [18], the covariance matrix of a uniform array can be estimated by that of a non-uniform array containing some of the same sensors. Consider a $V \times V$ URA, where $V = M_1M_2 - M_1 + 1$. This is the same size as the coprime planar array. And we define the set as $\widetilde{L} = \{(m,n), 0 \le m, n \le V-1\}$. Under the same situations, the covariance matrix without the noise is defined as $\widetilde{R}$, and the element in the mth row and th column is expressed as

$$\widetilde{R}_{m,n} = \sum_{k=1}^{K} \sigma_k^2 e^{j\pi \sin\theta_k((x_m - x_n)\cos\varphi_k + (y_m - y_n)\sin\varphi_k)} = \widetilde{R}(x_m - x_n, y_m - y_n), \tag{9}$$

where the (x_m, y_m) is one element of set $\widetilde{L}$. Thus, we define the two sets as

$$R_{Diff} = \{(x_m - x_n, y_m - y_n) | (x_m, y_m), (x_n, y_n) \in L\} \tag{10}$$

$$\widetilde{R}_{Diff} = \left\{(x_m - x_n, y_m - y_n) \middle| (x_m, y_m), (x_n, y_n) \in \widetilde{L}\right\} \tag{11}$$

For $M_1 = 3$ and $M_2 = 4$, Figure 2 shows the values in R_{Diff} and $\widetilde{R}_{Diff}$. The figure shows that all elements of R_{Diff} are included in $\widetilde{R}_{Diff}$. Accordingly, we can use R to estimate $\widetilde{R}$. However, some elements of $\widetilde{R}_{Diff}$ do not exist in R_{Diff}. If we reduce the aperture of the uniform array, we can estimate all elements, with some loss of accuracy. As a result, we estimate $\widetilde{R}$ with the values of R and tentatively set the uncertain values to zeros.

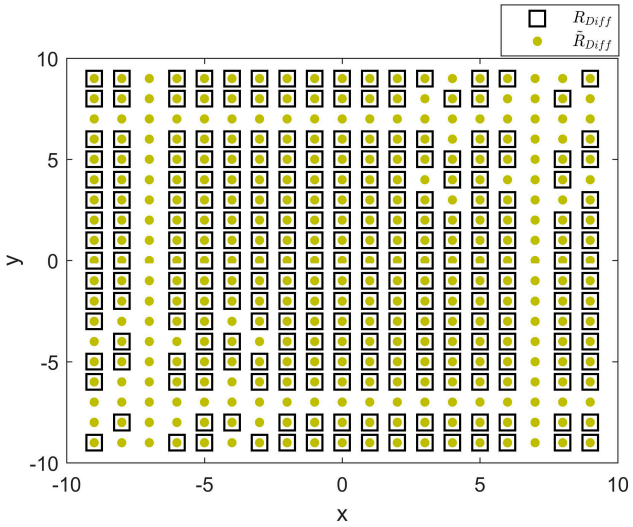

Figure 2. Values of sets R_{Diff} and $\widetilde{R}_{Diff}$ when $M_1 = 3, M_2 = 4$.

In practice, the theoretical covariance matrix given by (7) is unavailable because the number of snapshots is limited. Instead, it is usually estimated as

$$\hat{R}_X = \frac{1}{J} X X^H \tag{12}$$

Hence, $\hat{R}_X$ replaces R and the estimated covariance matrix of the virtual URA is defined as $\hat{R}_V$.

3.2. Matrix Completion Theory

It has been found that the virtual ULA transformed from the one-dimensional coprime array has holes [19,20], but these assertions used convex optimization to estimate the zero-location values in the covariance matrix of virtual array under the condition that the hole values were zeros. Similarly, the matrix completion theory [21] can be introduced to estimate the zeros of $\hat{R}_V$.

Firstly, the problem is rewritten as

$$\begin{aligned} &\min \quad rank(R_C) \\ &s.t \quad P_\Omega\ (R_C) = P_\Omega\left(\hat{R}_V\right) \end{aligned}, \tag{13}$$

where R_C is the target matrix and P_Ω is the sampling operator. The values of P_Ω are denoted as the sampling location of one matrix. If $P_\Omega = \{(m-1)V + n, 1 \le m, n \le V\}$, we can set the values in the mth row and the nth column of a $V \times V$ target matrix (initializing the target matrix as null matrix) as that in same location of matrix operated. Once the structure of the coprime planar array has been determined, the location of the non-zero elements, represented by P_Ω, is uniquely determined. As R_C is low rank, we estimate the zero-location values by requiring the rank of the target matrix to be as low as possible. Solving the rank minimization is NP-hard, so we need to employ a convex relaxation method. Singular value thresholding (SVT) [21,22] is a computationally effective method that offers fast convergence. Given [22], SVT is a nuclear norm minimization approach and converts (13) to

$$\begin{aligned} &\min \mu \|R_C\|_* + \tfrac{1}{2}\|R_C\|_F^2 \\ &s.t. \|P_\Omega(R_C) - \hat{R}_V\|^2 \le \varepsilon_0 \end{aligned}, \tag{14}$$

where μ is a constant, ε_0 is a constraint on the noise power, and $\|R_C\|_* = \sum_{i=1}^{n} \lambda_i(R_C)$, where $\lambda_i(R_C)$ denotes the ith singular value of R_C. The steps of the SVT algorithm are presented as follows:

Step 1: Choose appropriate values of μ, δ, ε and then initialize $R_S^0 = \hat{R}_V$;

Step 2: Calculate the $R_C^i = F_\mu\left(R_S^{i-1}\right)$ on the ith iteration;

Step 3: Update $R_S^i = R_S^{i-1} + \delta(\hat{R}_V - P_\Omega(R_C^i))$;

Step 4: If $\|P_\Omega(R_C^i) - \hat{R}_V\|_F^2 / \|\hat{R}_V\|_F > \varepsilon$, let $i = i + 1$ and return to step 2. If not, define $R_C = R_C^i$.

We call $F_\mu(R_S)$ a soft threshold operator. This is defined as

$$F_\mu(R_S) = UF(\textstyle\sum)V^H, \tag{15}$$

where $R_S = U\sum V^H; \sum = diag\begin{pmatrix} \lambda_1 & \cdots & \lambda_M \end{pmatrix}$ and λ_i represents ith singular value arranged from low to high; $F(\sum) = diag\begin{pmatrix} \widetilde{\lambda}_1 & \cdots & \widetilde{\lambda}_M \end{pmatrix}$, where

$$\widetilde{\lambda}_i = \begin{cases} \lambda_i - \mu & \lambda_i \geq \mu \\ 0 & \lambda_i < \mu \end{cases} \tag{16}$$

In [22], the values of μ, δ, ε are considered; we set them as $\mu = 5(M_1M_2 - M_1 + 1)^2$, $\delta = 1.21$ and $\varepsilon = 10^{-3}$, respectively. Finally, we obtain the covariance matrix of the virtual array by estimating the zero-location value of.

Before estimating DOAs, we need to know the number of signals, which is essential for accurate DOA estimation. Hence, we assume that the signal number is known. However, a method to detect more signals than the number of sensors is presented in [23,24], and the rank of matrix estimated by the algorithms is equal to the number of signals. All three methods aim to estimate a low rank matrix based on nuclear norm minimization. But the proposed algorithm is applied to a more complicated model, where the results are not only affected by the noise, but also by zero-value elements of $\hat{R}_V$. In spite of this, we can still use matrix completion to estimate the number of signals, and it would we worthwhile to analyze the relationship between the number of signals and the rank of R_C in further research.

Generally, we apply the 2D-MUSIC algorithm to find the azimuth and elevation angle of signals. From [25], the spatial spectrum function of angles is given by

$$P(\varphi, \theta) = \|U_n^H \widetilde{a}(\varphi, \theta)\|_2^{-2}, \tag{17}$$

where U_n is the noise subspace of R_C given by eigenvalue decomposition. $\widetilde{a}(\varphi, \theta)$ is expressed as

$$\widetilde{a}(\varphi, \theta) = \begin{bmatrix} \widetilde{a}_1(\varphi, \theta) & \widetilde{a}_2(\varphi, \theta) & \cdots & \widetilde{a}_{V^2}(\varphi, \theta) \end{bmatrix}^T, \tag{18}$$

where $\widetilde{a}_m(\varphi, \theta) = e^{j\pi \sin\theta(x_m \cos\varphi + y_m \sin\varphi)}, (x_m, y_m) \in \widetilde{L}$. In the spectral peak search, the angles corresponding to the peaks are the estimated values $(\hat{\varphi}_i, \hat{\theta}_i)$.

3.3. Unitary-ESPRIT Algorithm

Although 2D-MUSIC can find the DOAs, its total angular field-of-view search is computationally expensive. We construct the URA so that we can introduce the Unitary-ESPRIT [26,27] to give the fast estimations without paring parameters.

First, we define the inverse matrix $\prod_k$, whose counter-diagonal values are 1 while the other are 0, as $(\prod_k)^2 = \mathrm{I}_k$. The unitary matrix is defined to satisfy

$$\prod_k Q^* = Q \tag{19}$$

Moreover, the matrix can be expressed as

$$Q_{2k} = \frac{1}{\sqrt{2}} \begin{bmatrix} \mathrm{I}_k & j\mathrm{I}_k \\ \prod_k & -j\prod_k \end{bmatrix} \tag{20}$$

$$Q_{2k+1} = \frac{1}{\sqrt{2}} \begin{bmatrix} \mathrm{I}_k & \mathrm{O} & j\mathrm{I}_k \\ T & \sqrt{2} & T \\ \Pi_k & \mathrm{O} & -j\Pi_k \end{bmatrix} \tag{21}$$

The selection matrix is then $J_1 = \begin{bmatrix} I_{M+N-1} & O \end{bmatrix}$ and $J_2 = \begin{bmatrix} O & I_{M+N-1} \end{bmatrix}$. Define

$$K_1 = Re\left\{ Q_{M+N-1}^H J_2 Q_{M+N}^H \right\} \tag{22}$$

$$K_2 = \mathrm{Im}\left\{ Q_{M+N-1}^H J_2 Q_{M+N}^H \right\} \tag{23}$$

Therefore, we have

$$K_{\mu 1} = I_{M+N} \otimes K_1 \tag{24}$$

$$K_{\mu 2} = I_{M+N} \otimes K_2 \tag{25}$$

$$K_{\nu 1} = K_1 \otimes I_{M+N} \tag{26}$$

$$K_{\nu 2} = K_2 \otimes I_{M+N} \tag{27}$$

Next, we transform R_T to give

$$R_T = Re\left\{ \left(Q_V^H \otimes Q_V^H \right) R_C \left(Q_V^H \otimes Q_V^H \right)^H \right\}, \tag{28}$$

where R_T is a real-valued matrix. The eigenvalue decomposition of a real matrix is less complex than that of a complex matrix, and we can obtain the signal subspace U_S. Finally, we take the last two steps into consideration and obtain

$$\psi_\mu = \left(K_{\mu 1} U_S \right)^+ K_{\mu 2} U_S \tag{29}$$

$$\psi_\nu = \left(K_{\nu 1} U_S \right)^+ K_{\nu 2} U_S \tag{30}$$

Define $\psi = \psi_\mu + j\psi_\nu$ and take the eigenvalue decomposition to acquire the eigenvalue vector λ. We have

$$\hat{\theta}_i = \arcsin\left(\sqrt{(\mu_i/\pi)^2 + (\nu_i/\pi)^2} \right) \tag{31}$$

$$\hat{\varphi}_i = \arctan(\nu_i/\mu_i), \tag{32}$$

where $(\hat{\varphi}_i, \hat{\theta}_i)$ is the estimated value, $\mu_i = 2\arctan\left((\lambda_i + \lambda_i^*)/2 \right)$, and $\nu_i = 2\arctan\left((\lambda_i - \lambda_i^*)/2 \right)$. The Unitary-ESPRIT algorithm gives the closed-form solutions of DOAs, thus avoiding the spectral peak search.

3.4. Algorithm Steps Conclusion

The main steps of the proposed algorithm can be summarized as follows:

Step 1: Calculate the received signals' covariance matrix $\hat{R}_X$.

Step 2: Given $\hat{R}_X$, estimate the covariance matrix $\hat{R}_V$ of the virtual uniform array combined with the array structure.

Step 3: Apply the matrix completion theory to estimate the zero-location elements of $\hat{R}_V$ and obtain R_C.

Step 4: Use the Unitary-ESPRIT algorithm to solve for the estimated DOA values $(\hat{\varphi}_i, \hat{\theta}_i)$.

4. Computational Complexity and Freedom Degree Analysis

4.1. Complexity Analysis

The computational complexity of the proposed algorithm using Unitary-ESPRIT is made up of four parts: covariance matrix estimation, SVT, eigenvalue decomposition and Unitary-ESPRIT. The complexities of these four parts are $O(JM^2)$, $O\left(\left(4K\sqrt{K} + 8\left(\sqrt{K} \right)^3 \right) N_t \right)$, $O\left(\left(V^2 \right)^3 \right)$,

and $O\left(\left(2V^2\right)^3 + K^3\right)$, respectively, where N_t denotes the iterations number and $V = M_1M_2 - M_1 + 1$. Therefore, the computational complexity of the proposed algorithm is given as $O\left(JM^2 + \left(4K\sqrt{K} + 8\left(\sqrt{K}\right)^3\right)N_t + K^3 + 9V^6\right)$. After reconstructing the virtual URA, 2D-MUSIC can also be used to estimate DOAs, and the complexity of the spectral peak search method is $O\left(V^2\left(V^2 - K\right)G_\varphi G_\theta\right)$, where G_φ, G_θ represent the number of spectral points of the total field-of-view. Hence, the computational complexity of proposed algorithm applying 2D-MUSIC is given as $O\left(JM^2 + \left(4K\sqrt{K} + 8\left(\sqrt{K}\right)^3\right)N_t + V^6 + V^2\left(V^2 - K\right)G_\varphi G_\theta\right)$. Moreover, the complexity of the PSS method [15] is $O\left(J\left(M_1^4 + M_2^4\right) + M_1^6 + M_2^6 + G_\varphi G_\theta\left(\frac{M_1^4}{M_2^2} + \frac{M_2^4}{M_1^2}\right)\right)$. For the sake of clarity, the computational complexity of all these methods is summarized in Table 1. We also compare the complexity of methods versus snapshots (J), the number of sensors (M) and the searching step ($\Delta\theta = \Delta\varphi$, where $G_\theta = 90/\Delta\theta, G_\varphi = 360/\Delta\varphi$) in Figure 3a–c, respectively.

Table 1. Computational Complexity Comparison of Different Algorithms.

Algorithms	Complexity
Unitary-ESPRIT	$O\left(JM^2 + 12K\sqrt{K}N_t + K^3 + 9V^6\right)$
2D-MUSIC	$O\left(JM^2 + 12K\sqrt{K}N_t + V^6 + V^2\left(V^2 - K\right)G_\varphi G_\theta\right)$
PSS	$O\left(J\left(M_1^4 + M_2^4\right) + M_1^6 + M_2^6 + G_\varphi G_\theta\left(\frac{M_1^4}{M_2^2} + \frac{M_2^4}{M_1^2}\right)\right)$

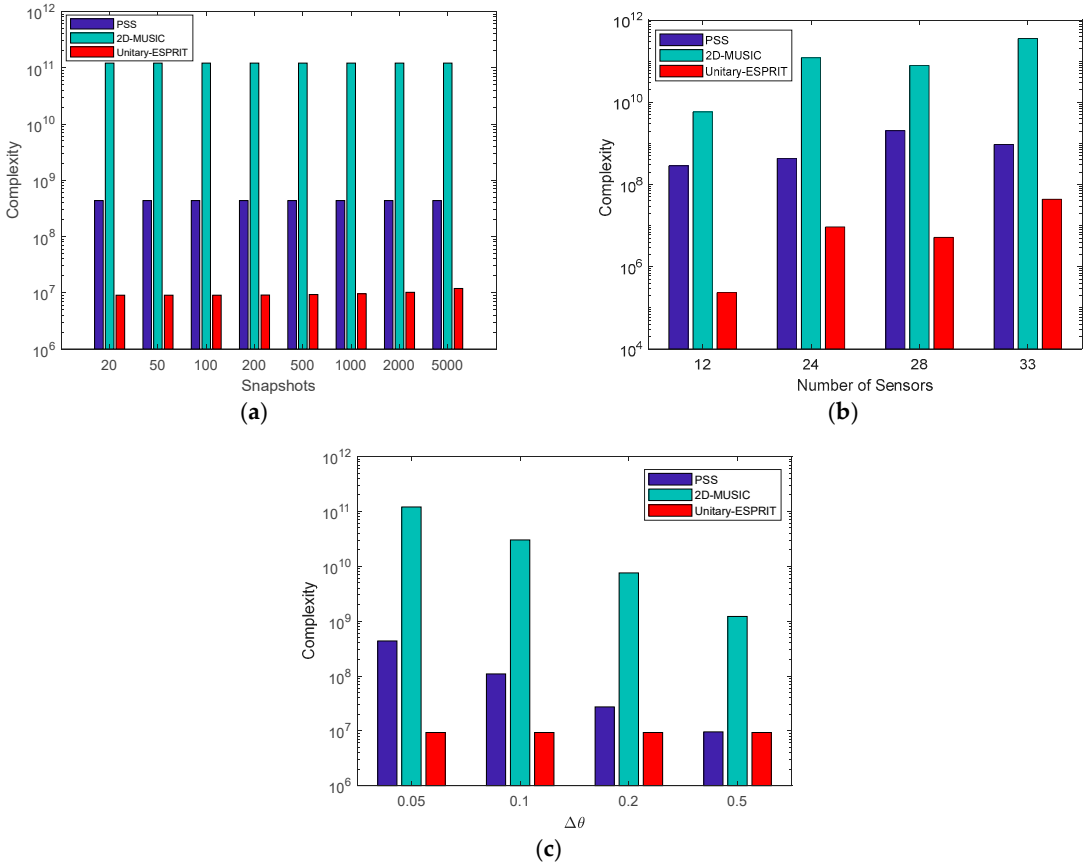

Figure 3. Complexity comparison (**a**) versus snapshots when $M_1 = 3, M_2 = 4, \Delta\theta = 0.05^\circ$; (**b**) versus the number of sensors when $J = 500, \Delta\theta = 0.05^\circ$; (**c**) versus the searching step when $M_1 = 3, M_2 = 4, J = 500$.

As shown in Figure 3, Unitary-ESPRIT has the smallest complexity. The number of snapshots has a weak impact on complexity, while the searching step has the strongest impact. The PSS method and the proposed algorithm using 2D-MUSIC are both based on a 2D search, which means that the complexity is high when the searching step is small. Therefore, we introduce the Unitary-ESPRIT algorithm to replace the search methods and provide the closed-form solutions for the DOAs. Hence, the searching step does not affect the complexity of the proposed algorithm using Unitary-ESPRIT. The main component of the computational complexity in the proposed algorithm is SVT, where the iteration number is, on average, 200. However, compared with the search methods, the complexity is relatively low. As a result, the proposed algorithm can reduce complexity to realize fast estimations.

4.2. Freedom Degree Analysis

The degree of freedom is affected by the array and the algorithm that we choose, and determines the maximum number of signals that we can estimate directly. The algorithms presented in [15] and [17] have freedom degrees of $O(M_1^2 - 1)$ and $O((M^2 - 1)/8)$, respectively. The proposed algorithm reconstructs a $V \times V$ virtual URA based on the coprime planar array with the M sensors number. The Unitary-ESPRIT or 2D-MUSIC used to estimate DOAs has no influence to degree of freedom, and each one obtains a degree of freedom of $O(V^2 - 1)$. The detailed values are presented in Figure 4. The freedom degree of the algorithm in [15] depends on M_1, so it is the lowest, while that of the URA is no more than the number of sensors. Both the proposed algorithm and the method introduced in [17] have freedom degrees that are greater than the number of sensors. Comparing the two algorithms, we find that the proposed algorithm has a higher degree of freedom. Thus, we have developed an algorithm using coprime planar arrays that offers a high degree of freedom, enabling multiple signals to be resolved.

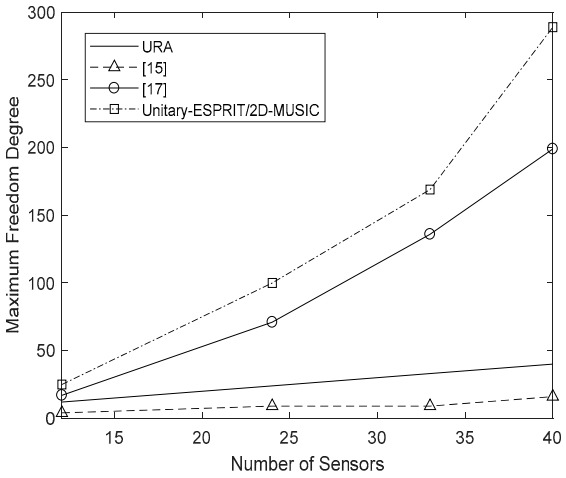

Figure 4. Freedom degree versus the number of sensors.

5. Simulation Results

This section reports the results of performance simulation experiments comparing the proposed algorithm using Unitary-ESPRIT with that using 2D-MUSIC [25] and the PSS method [15]. To measure the accuracy of the algorithms, we define the root mean square error (RMSE) as

$$\text{RMSE} = \sqrt{\frac{1}{QK}\sum_{i=1}^{Q}\|\gamma - \hat{\gamma}_i\|^2} \tag{33}$$

where Q denotes the number of simulation; γ and $\hat{\gamma}_i$ are defined as the real values and the ith estimated values, respectively. We assume that $M_1 = 3, M_2 = 4$, and then have $M = 24$, $V = 10$.

Simulation 1: Performance under the condition of multiple signals ($K > M$).

We consider the cases of $K = 25$ or $K = 30$ signals with a signal-to-noise ratio (SNR) of 10 dB, $J = 500$ and $\Delta\theta = \Delta\varphi = 0.05°$. The spatial spectrum contour map of the total field-of-view is shown in Figure 5, as given by 2D-MUSIC algorithm. The distribution of the estimated values from 20 simulations using the Unitary-ESPRIT algorithm is presented in Figure 6. Figure 5 shows that we can find the 25 or 30 peaks, and proves that the proposed method using 2D-MUSIC can solve problems in which the number of signals is greater than the number of sensors. Moreover, Figure 6 shows that the proposed algorithm using Unitary-ESPRIT gives estimated values that are close to the real values over 20 simulations, indicating robust performance. Compared with the PSS method, which finds at most M_1^2 signals, we make better use of the high freedom degree to estimate more signal directions.

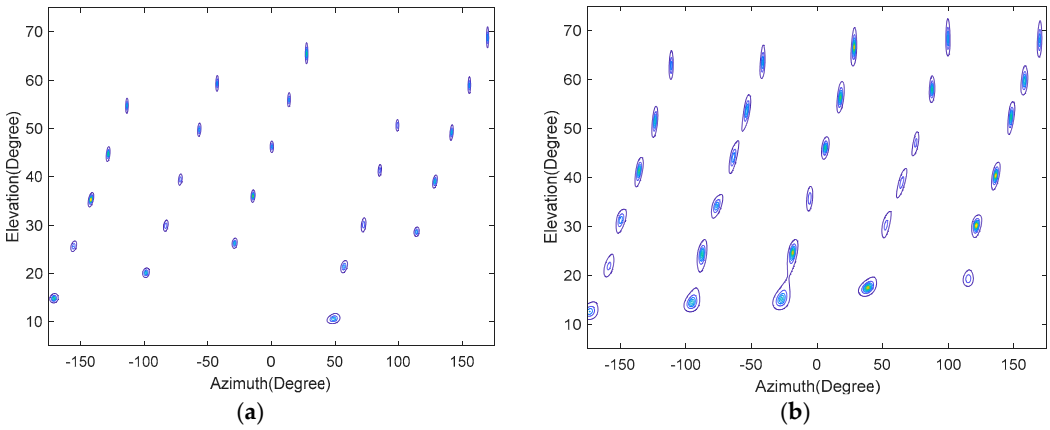

Figure 5. Spatial spectrum contour map (**a**) $K = 25$ (**b**) $K = 30$.

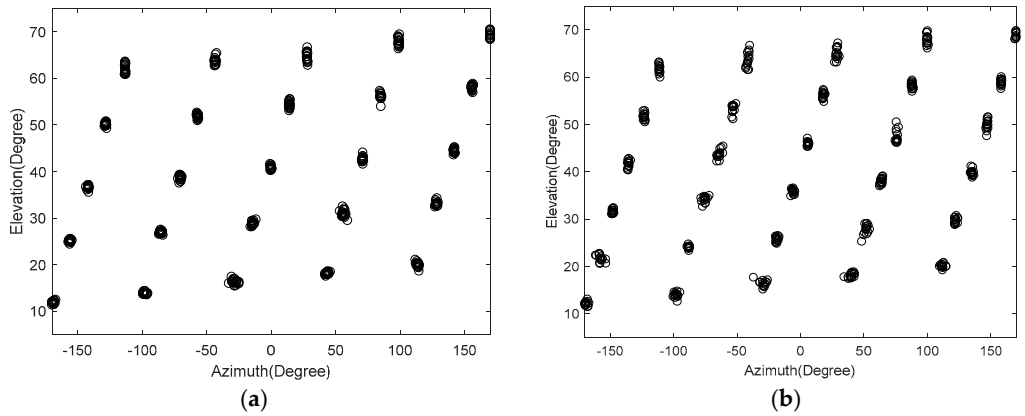

Figure 6. Distribution of azimuth and elevation estimation (**a**) $K = 25$ (**b**) $K = 30$.

Simulation 2: RMSE comparison of the proposed algorithm using Unitary-ESPRIT and 2D-MUSIC, the PSS method, and the URA with the same number of sensors under different SNRs.

Simulations are conducted with $Q = 100$, $J = 500$ and SNRs from -5 dB to 15 dB at 5 dB intervals. And we set $K = 7, \Delta\theta = \Delta\varphi = 0.5°$, $K = 7, \Delta\theta = \Delta\varphi = 0.05°$ and $K = 10, \Delta\theta = \Delta\varphi = 0.05°$. The RMSE results are shown in Figures 7–9, respectively.

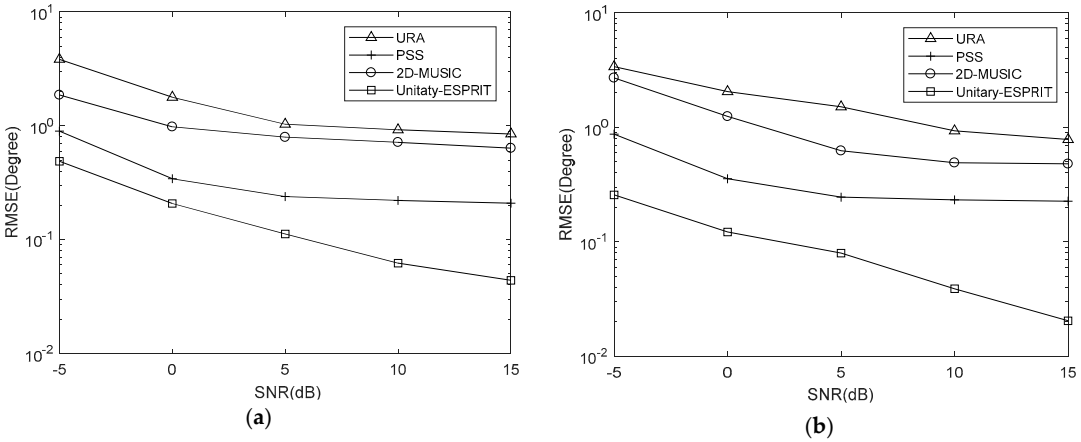

Figure 7. RMSE comparison under different SNRs with $K = 7, \Delta\theta = \Delta\varphi = 0.5^\circ$ (**a**) azimuth (**b**) elevation.

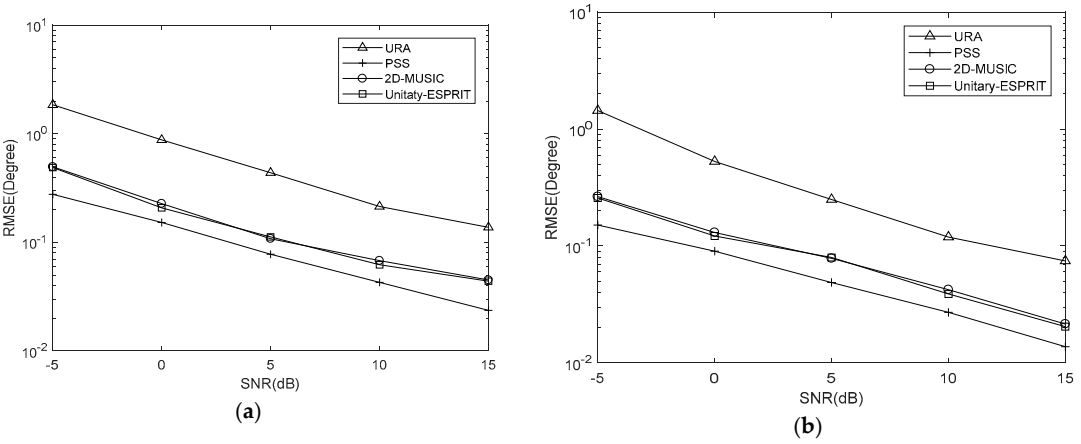

Figure 8. RMSE comparison under different SNRs with $K = 7, \Delta\theta = \Delta\varphi = 0.05^\circ$ (**a**) azimuth (**b**) elevation.

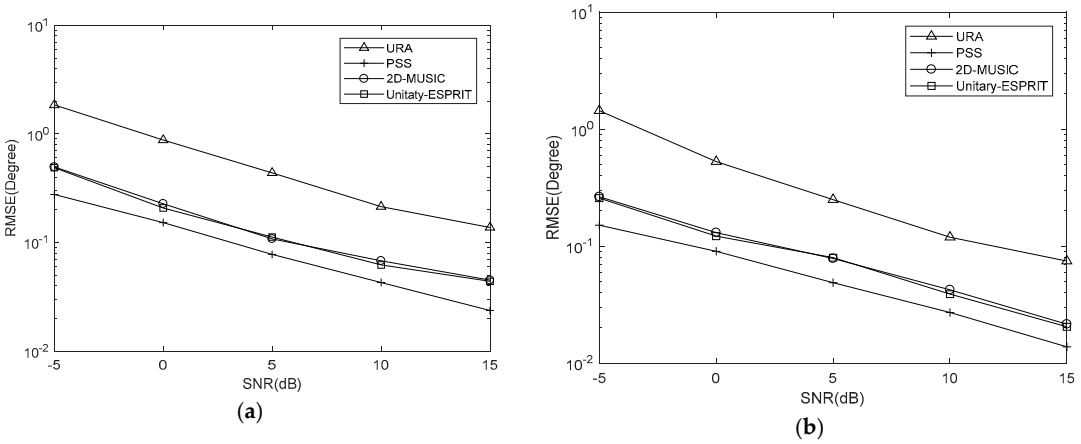

Figure 9. RMSE comparison under different SNRs with $K = 10, \Delta\theta = \Delta\varphi = 0.05^\circ$ (**a**) azimuth (**b**) elevation.

It is evident that the RMSE of the coprime planar array is lower than that of URA with the same number of sensors. This is because the coprime planar array has a bigger array aperture when the number of sensors is known. The RMSEs of the proposed algorithm using 2D-MUSIC and PSS are affected by the searching step, while that of proposed algorithm using Unitary-ESPRIT

are not. The former two methods can obtain the lower RMSE when the searching step is smaller. The results verify that Unitary-ESPRIT has lower RMSE than 2D-MUSIC when $\Delta\theta = \Delta\varphi = 0.5^\circ$. But 2D-MUSIC gives a similar RMSE to Unitary-ESPRIT when $\Delta\theta = \Delta\varphi = 0.05^\circ$. Given the results of our complexity analysis, 2D-MUSIC obtains similarly precise estimations as Unitary-ESPRIT at the cost of higher complexity.

When $K = 7, \Delta\theta = \Delta\varphi = 0.05^\circ$, the PSS method is effective and outperforms the proposed algorithm using Unitary-ESPRIT. There are two reasons for this. One is the searching step of PSS is small. The other is the covariance matrix of virtual URA is estimated by SVT, which introduces errors to the covariance matrix. But the PSS calculates the covariance matrix of coprime planar array directly, without additional methods. However, when $K = 7, \Delta\theta = \Delta\varphi = 0.5^\circ$ and $K = 10, \Delta\theta = \Delta\varphi = 0.05^\circ$, the PSS method has the higher RMSE than proposed algorithm using Unitary-ESPRIT, and fails; however, Unitary-ESPRIT maintains its accuracy. Although the PSS can have lowest RMSE, it may come at the cost of higher complexity. And when applied to multiple signals, the proposed algorithm using Unitary-ESPRIT is preferable and offers real-time performance due to the minimal complexity.

Simulation 3: RMSE comparison of the proposed algorithm using Unitary-ESPRIT and 2D-MUSIC, the PSS method and the URA with the same number of sensors under different number of snapshots.

In simulation 3, we set the SNR to 15 dB and varied the number of snapshots to $J = [20, 50, 100, 200, 500, 1000, 2000, 5000]$. The results are presented in Figures 10–12. The RMSE decreases as the number of snapshots increases, although the decline is negligible once $J > 500$. The conclusions of simulation 2 are also applicable to the number of snapshots.

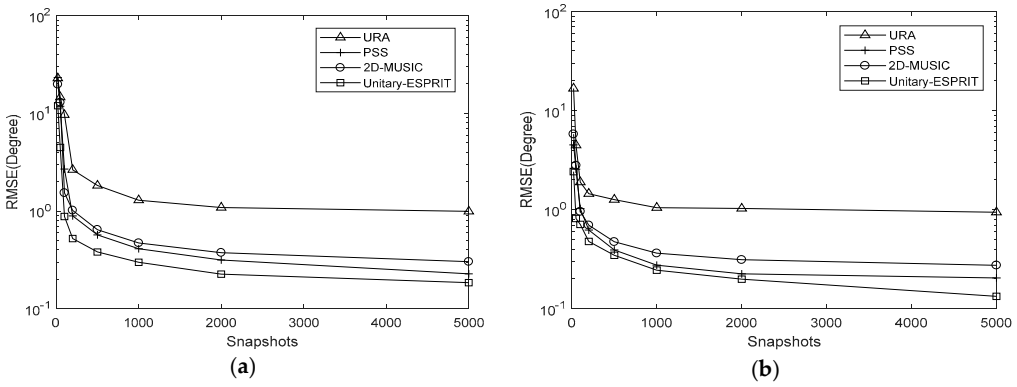

Figure 10. RMSE comparison under different snapshots with $K = 7, \Delta\theta = \Delta\varphi = 0.5^\circ$ (**a**) azimuth (**b**) elevation.

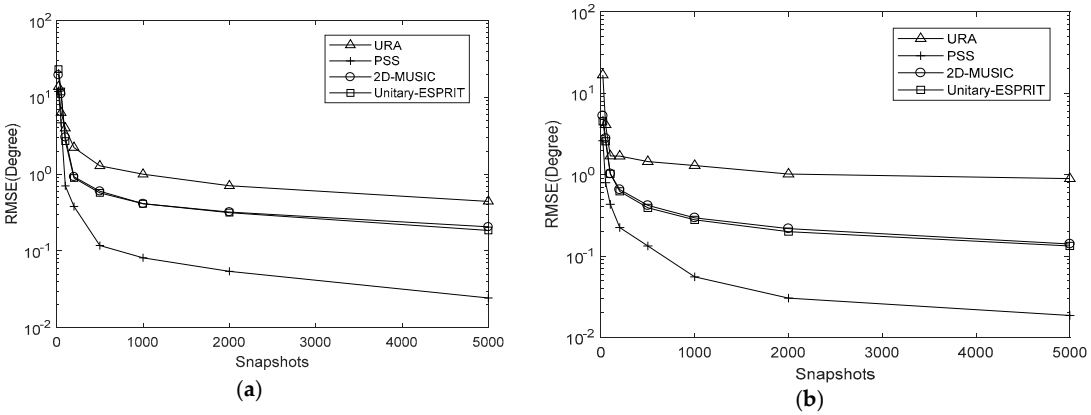

Figure 11. RMSE comparison under different snapshots with $K = 7, \Delta\theta = \Delta\varphi = 0.05^\circ$ (**a**) azimuth (**b**) elevation.

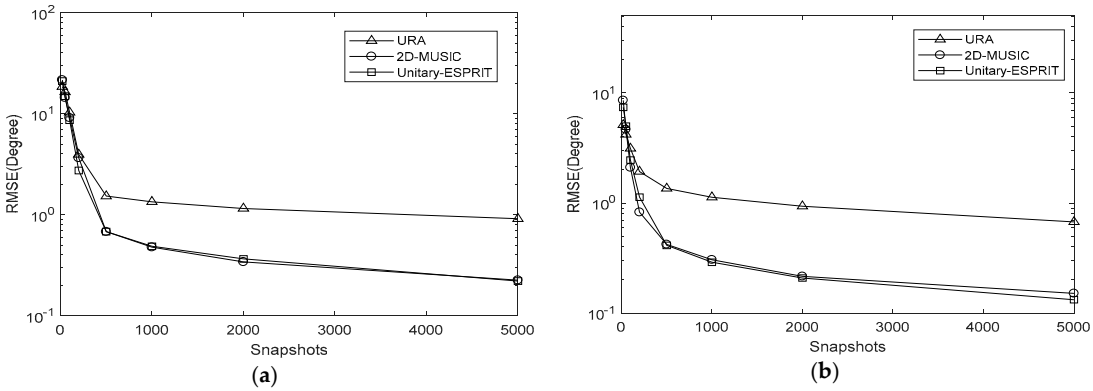

Figure 12. RMSE comparison under different snapshots with $K = 10, \Delta\theta = \Delta\varphi = 0.05^\circ$ (**a**) azimuth (**b**) elevation.

6. Conclusions

This paper has presented a DOA estimation technique for multiple signals using a coprime planar array. Using matrix completion theory combined with the Unitary-ESPRIT algorithm, the proposed technique overcomes the problems of existing algorithms, namely the high computational complexity of the 2D spectral peak search and an inability to find more signals than the number of sensors. This paper has described the model and the associated algorithm, and analyzed the computational complexity of the proposed algorithm in comparison with that of existing algorithms. Through theoretical analysis and a series of simulation experiments, we can conclude that the proposed algorithm attains higher accuracy than URA with the same number of sensors. Using the matrix completion theory to estimate the covariance matrix of a virtual URA, we can obtain a better degree of freedom to find multiple signals. Furthermore, applying the Unitary-ESPRIT algorithm to find the closed-form DOA solution greatly reduces the computational complexity.

Author Contributions: H.X. proposed the main idea and analyzed the algorithm with Y.Z. and X.L.; H.X. designed the simulations and analyzed the results with Y.Z. and B.B.; H.X. wrote the paper under the guidance of B.B. and D.W.; X.L. has critically reviewed the paper. All authors read and approved the final manuscript.

Funding: The work was supported by the National Natural Science Foundation of China (grant no. 61401513).

Conflicts of Interest: The authors declare no conflict of interest.

References

1. Wei, X.; Liu, Z.; Ding, X.; Fan, M. Super-Resolution Reconstruction of Radar Tomographic Image Based on Image Decomposition. *IEEE Geosci. Remote Sens. Lett.* **2013**, *11*, 607–611.
2. Wang, Y.L.; Ma, S.L.; Liang, G.L.; Fan, Z. Chirp Spread Spectrum of Orthogonal Frequency Division Multiplexing Underwater Acoustic Communication System Based on Multi-path Diversity Receive. *Acta Phys. Sin.* **2014**, *63*. [CrossRef]
3. Gao, Z.; Dai, L.; Lu, Z.; Wang, Z. Super-resolution Sparse MIMO-OFDM Channel Estimation Based on Spatial and Temporal Correlations. *IEEE Commun. Lett.* **2014**, *18*, 1266–1269. [CrossRef]
4. Ye, Z.; Dai, J.; Xu, X.; Wu, X. DOA Estimation for Uniform Linear Array with Mutual Coupling. *IEEE Trans. Aerosp. Electron. Syst.* **2009**, *45*, 280–288.
5. Heidenreich, P.; Zoubir, A.M.; Rubsamen, M. Joint 2-D DOA Estimation and Phase Calibration for Uniform Rectangular Arrays. *IEEE Trans. Signal Process.* **2012**, *60*, 4683–4693. [CrossRef]
6. Han, H.; Zhao, P.J. A Two-dimensional direction finding estimation with L-shape uniform linear arrays. In Proceedings of the International Symposium on Instrumentation and Measurement, Sensor Network and Automation, Toronto, ON, Canada, 23–24 December 2013; IEEE: Piscataway, NJ, USA, 2014; pp. 779–782.

7. Pal, P.; Vaidyanathan, P.P. Coprime sampling and the music algorithm. In Proceedings of the 2011 IEEE Digital Signal Processing Workshop and IEEE Signal Processing Education Workshop, Sedona, AZ, USA, 4–7 January 2011; pp. 289–294.
8. Zhang, D.; Zhang, Y.; Zheng, G.; Feng, C.; Tang, J. Improved DOA Estimation Algorithm for Co-prime Linear Arrays Using Root-MUSIC Algorithm. *Electron. Lett.* **2017**, *53*, 1277–1279. [CrossRef]
9. Zhou, C.; Zhou, J. Direction-of-Arrival Estimation with Coarray ESPRIT for Coprime Array. *Sensors* **2017**, *17*. [CrossRef]
10. Byun, B.G.; Yoo, D.S. Improved Direction of Arrival Estimation Based on Coprime Array and Propagator Method by Noise Power Spectral Density Estimation. *J. Adv. Nav. Tech.* **2016**, *20*, 367–373. [CrossRef]
11. Dai, Z.-L.; Cui, W.-J.; Ba, B.; Zhang, Y.-K. Two-dimensional Direction-of-arrival Estimation of Coherently Distributed Noncircular Signals via Symmetric Shift Invariance. *Acta Phys. Sin.* **2017**, *66*, 220701. [CrossRef]
12. Ba, B.; Liu, G.-C.; Li, T.; Lin, Y.-C.; Wang, Y. Joint for Time of Arrival and Direction of Arrival Estimation Algorithm Based on the Subspace of Extended Hadamard Product. *Acta Phys. Sin.* **2015**, *64*, 078403. [CrossRef]
13. Pal, P.; Vaidyanathan, P.P. Nested Arrays: A Novel Approach to Array Processing with Enhanced Degrees of Freedom. *IEEE Trans. Signal Process.* **2010**, *58*, 4167–4181. [CrossRef]
14. Vaidyanathan, P.P.; Pal, P. Sparse Sensing With Co-Prime Samplers and Arrays. *IEEE Trans. Signal Process.* **2011**, *59*, 573–586. [CrossRef]
15. Wu, Q.; Sun, F.; Lan, P.; Ding, G.; Zhang, X. Two-Dimensional Direction-of-Arrival Estimation for Co-Prime Planar Arrays: A Partial Spectral Search Approach. *IEEE Sens. J.* **2016**, *16*, 5660–5670. [CrossRef]
16. Liu, S.; Yang, L.; Li, D.; Cao, H. Subspace Extension Algorithm for 2D DOA Estimation with L-shaped Sparse Array. *Multidimens. Syst. Signal Process.* **2017**, *28*, 315–327. [CrossRef]
17. Qin, S.; Zhang, Y.D.; Amin, M.G. Two-dimensional DOA estimation using parallel coprime subarrays. In Proceedings of the 2016 IEEE Sensor Array and Multichannel Signal Processing Workshop, Rio de Janerio, Brazil, 10–13 July 2016.
18. Pillai, S.; Haber, F. Statistical Analysis of a High Resolution Spatial Spectrum Estimator Utilizing an Augmented Covariance Matrix. *IEEE Trans. Acoust. Speech Signal Process.* **1987**, *35*, 1517–1523. [CrossRef]
19. Chen, T.; Guo, M.; Guo, L. A Direct Coarray Interpolation Approach for Direction Finding. *Sensors* **2017**, *17*, 2149. [CrossRef] [PubMed]
20. Guo, M.; Chen, T.; Wang, B. An Improved DOA Estimation Approach Using Coarray Interpolation and Matrix Denoising. *Sensors* **2017**, *17*, 1140. [CrossRef] [PubMed]
21. Wu, C.X.; Zhang, M.; Wang, K.R. An Underdetermined DOA Estimation Approach in Coprime Array Based on Matrix Completion. *J. Sichuan Univ. Eng. Sci. Ed.* **2017**, *49*, 156–163.
22. Cai, J.F.; Candes, E.J.; Shen, Z.W. A Singular Value Thresholding Algorithm for Matrix Completion. *SIAM J. Optim.* **2010**, *4*, 1956–1982. [CrossRef]
23. Pal, P.; Vaidyanathan, P.P. A Grid-Less Approach to Underdetermined Direction of Arrival Estimation via Low Rank Matrix Denoising. *IEEE Signal Process. Lett.* **2014**, *21*, 737–741. [CrossRef]
24. Sun, F.; Wu, Q.; Lan, P.; Ding, G.; Chen, L. Real-Valued DOA Estimation with Unknown Number of Sources via Reweighted Nuclear Norm Minimization. *Signal Process.* **2018**, *148*, 48–55. [CrossRef]
25. Chen, Y.M.; Lee, J.H.; Yeh, C.C. Two-dimensional Angle-of-arrival Estimation for Uniform Planar Arrays with Sensor Position Errors. *IEE Proc. F Radar Signal Process.* **1993**, *140*, 37–42. [CrossRef]
26. Haardt, M.; Nossek, J.A. Unitary ESPRIT: How to Obtain Increased Estimation Accuracy with a Reduced Computational Burden. *IEEE Trans. Signal Process.* **1995**, *43*, 1232–1242. [CrossRef]
27. Zoltowski, M.D.; Haardt, M.; Mathews, C.P. Closed-form 2-D Angle Estimation with Rectangular Arrays in Element Space or Beamspace via Unitary ESPRIT. *IEEE Trans. Signal Process.* **1996**, *44*, 316–328. [CrossRef]